

# Large-Scale Network Simulation Techniques: Examples of TCP and OSPF Models <sup>\*</sup>

Garrett R. Yaun<sup>†</sup>, David Bauer<sup>†</sup>, Harshad L. Bhutada<sup>‡</sup>,  
Christopher D. Carothers<sup>†</sup>, Murat Yuksel<sup>‡</sup>, and Shivkumar Kalyanaraman<sup>‡</sup>

## ABSTRACT

Simulation of large-scale networks remains to be a challenge, although various network simulators are in place. In this paper, we identify fundamental issues for large-scale network simulation, and propose new techniques that address them. First, we exploit optimistic parallel simulation techniques to enable fast execution on inexpensive hyper-threaded, multiprocessor systems. Second, we provide a compact, light-weight implementation framework that greatly reduces the amount of state required to simulate large-scale network models. Based on the proposed techniques, we provide sample simulation models for two networking protocols: TCP and OSPF. We implement these models in a simulation environment ROSSNet, which is an extension to the previously developed optimistic simulator ROSS. We perform validation experiments for TCP and OSPF and present performance results of our techniques by simulating OSPF and TCP on a large and realistic topology, such as AT&T's US network based on Rocketfuel data. *The end result of these innovations is that we are able to simulate million node network topologies using inexpensive commercial off-the-shelf hyper-threaded multiprocessor systems consuming less than 1.4 GB of RAM in total.*

## Keywords

Large-Scale Network Simulation, TCP, OSPF, Optimistic synchronization protocol

## 1. INTRODUCTION

There is a deliberate need for large-scale simulation of various networking protocols in order to understand their dynamics. For example, there are several issues in routing that need to be under-

<sup>\*</sup>This research is supported by the DARPA's Network Modeling and Simulation program, contract #F30602-00-2-0537, NSF CAREER Award CCR-0133488, and AT&T Research.

<sup>†</sup>Department of Computer Science, 110 8th Street, Troy New York, 12180. (yaung, bauerd, chris)c@cs.rpi.edu

<sup>‡</sup>Department of Electrical and Computer Systems Engineering, 110 8th Street, Troy New York, 12180. (bhutada, yuksem, shivkuma)@ecse.rpi.edu

stood, such as cascading failures [1], inter/intra-domain routing stability, and interactions of policy-based routing with BGP features [2]. One needs to perform large-scale simulations of inter-domain routing protocols along with various traffic engineering extensions, in order to observe their dynamics causing or effecting various performance problems in the current Internet.

We address this need using two techniques. First, we leverage an optimistic synchronization protocol to enable efficient execution on a hyper-threaded, multiprocessor system. Here, simulation objects, such as a host or router, are allowed to process events unsynchronized without regard for the underlying topology or timestamp distribution. If an out-of-order event computation is detected, the simulation object is rolled back and re-processed in the correct timestamp order. Unlike previous optimistic protocols, such as Time Warp [3], the rollback mechanism is realized using *reverse computation*. Here, events are literally allowed to execute backward to undo the computation. This approach greatly reduces the amount of state required to support optimistic event processing as well as increases performance [4].

Next, we devise an extremely light-weight model implementation framework called ROSSNet that is specifically designed for large-scale network simulation. If we examine state-of-the-art frameworks, such as Ns[5], SSFNet [6], DaSSF [7] and PDNS [8], we find models that are highly detailed almost to the point of being full-protocol network emulators. For example, these frameworks provide support for a single end-host to have multiple interfaces, a full UNIX socket API for connecting to real applications, and other details that we believe are not necessarily relevant for large-scale simulation studies. The end result is that these systems require almost super-computer amounts of memory and processing power to execute large-scale models.

In contrast, our framework poses the question: *what do you really need to model in order to answer a particular protocol dynamics question in a large-scale scenario?* For example, are all layers in a protocol stack really necessary? Can a host just be a TCP sender or just a TCP receiver? Does the simulated host really need to be both? By asking these kinds of questions, our framework enables a single TCP connection to be realized in just 320 bytes total (both sender and receiver) and 64 bytes per each packet-event.

*These innovations enable the simulation of million node network topologies using inexpensive commercial off-the-shelf multiprocessor systems consuming less than 1.4 GB of RAM in total.*

The remainder of this article is organized as follows: Section 2,

provides a description of our simulation framework, ROSSNet, and parallel simulation engine, ROSS. Sections 3 and 4 describe the implementation of our TCP and OSPF models respectively. The results from our validation study for both models are presented in Section 5 followed by a performance study in Section 6. Section 7 describes related work and Section 8 presents the conclusions from this research and future work.

## 2. ROSS & ROSSNET

ROSS is an acronym for Rensselaer’s Optimistic Simulation System. It is a parallel discrete-event simulator that executes on shared-memory multiprocessor systems. ROSS is geared for running large-scale simulation models. Here, the optimistic simulator consists of a collection of *logical processes* or LPs, each modeling a distinct component of the system, such as a host or router. LPs communicate by exchanging timestamped event messages. Like most existing parallel/distributed simulation protocols, we assume LPs may not share state variables that are modified during the simulation. The synchronization mechanism must ensure that each LP processes events in timestamp order to prevent events in the simulated future from affecting those in the past. The Time Warp [3] mechanism uses a detection-and-recovery protocol to synchronize the computation. For the recovery, we employ a technique called *reverse computation*.

### 2.1 Reverse Computation

Under reverse computation, the roll back mechanism in the optimistic simulator is realized not by classic state-saving, but by literally allowing to the greatest possible extent events to be unprocessed in reverse order, effectively undoing the state changes. Thus, as models are developed for parallel execution, both the forward and reverse execution code must be written.

The key property that reverse computation exploits is that a majority of the operations that modify the state variables are “constructive” in nature. That is, the undo operation for such operations requires no history. Only the most current values of the variables are required to undo the operation. For example, operators such as  $++$ ,  $--$ ,  $+$ ,  $=$ ,  $-$ ,  $*$ ,  $=$  and  $/$ ,  $=$  belong to this category. Note, that the  $*$ ,  $=$  and  $/$ ,  $=$  operators require special treatment in the case of multiply or divide by zero, and overflow/underflow conditions. More complex operations such as *circular shift* (*swap* being a special case), and certain classes of random number generation also belong here [4].

Operations of the form  $a = b$ , modulo and bit-wise computations that result in the loss of data, are termed to be *destructive*. Typically these operations can only be restored using conventional state-saving techniques. However, we observe that many of these destructive operations are a consequence of the arrival of data contained within the event being processed. For example, in our TCP model, the last-sent time records the time stamp of the last packet forwarded on a router LP. We use the *swap* operation to make this operation reversible. We will show more examples of how this technique was used in our implementation of the TCP model below in Section 3.4.

### 2.2 ROSS Implementation

The ROSS API is kept very simple and lean. Developed in ANSIC, the API is based on a logical process or LP model. Services are provided to allocate and schedule messages between LPs. A random number generator library is provided based on L’Ecuyer’s

Combined Linear Congruential Generator[9]. Each LP by default is given a single seed set. All memory is directly managed by the simulation engine. Garbage or “fossil” collection, as defined in the seminal Time Warp research of Jefferson [3], is driven by the availability of free event memory. Fossil collection frequencies are controlled with tuning parameters and start-up memory allocation. The event-list priority queue can be configured to be either a Calendar Queue[10], Splay Tree [11] or a binary heap. For network models, the Splay Tree is considered to provide the best overall performance (i.e., is not sensitive to the event timestamp distribution).

To reduce garbage collection overheads, ROSS introduces kernel processes (KPs). A KP contains the statistics and processed event-list for a collection of LPs. With KPs there are fewer event-lists to search through during garbage collection, thereby improving performance, particularly when the number of LPs is large. For the experiments presented here we typically allocate 4 to 8 KPs per processor irrespective of the number of LPs. We observe KPs are similar to DaSSF timelines [7] and USSF clusters [12].

### 2.3 ROSSNet

By using ROSS as the simulation kernel, we are currently developing a network simulator called ROSSNet. Unlike conventional network simulators (e.g., Ns [5], JavaSim [13]) ROSSNet uses the flat programming environment of C rather than an object-oriented paradigm and leverages pointers to functions in the place of “virtual methods”. Here, developers set function pointers for both end hosts and routers alike to obtain the desired level of functionality. If a host is to behave like a TCP connection, it will set the event processing function for TCP, likewise if a router is forwarding packets based on either a static routing table or OSPF, it will set its function pointer appropriately.

Additionally, ROSSNet attempts to combine or reduce the event population and total number of events processed. For example, in the router model, both the forwarding plane and control plane functionality are all realized within the same logical process (LP). Thus, event processing on the control plane side, will immediately effect the forwarding plane without the need for explicit events to be passed between the two planes.

ROSSNet will also make use of global data structures. For example, in OSPF, each router maintains a map of the whole network. In simulation, this is not necessary. One can simply keep a global data structure in the simulation such that all the routers can reach it. This way redundant usage of memory is avoided.

Last, ROSSNet eliminates unnecessary layers of the protocol stack. For example, if one is interested in simulating behavior of a transport layer protocol, lower layers could be simplified such that they require less resources. This was done in our TCP model configuration.

Figure 1 shows the structure of ROSSNet. ROSSNet basically constructs a shell on top of the ROSS kernel, which handles system management issues such as event-list management, optimistic processing of events including rollback and recovery, and memory management. ROSSNet provides basic components for network simulation such as node, link, and queue. On top of these basic networking components, ROSSNet implements protocols such as OSPF and TCP. In this paper, we only present our OSPF and TCP models.

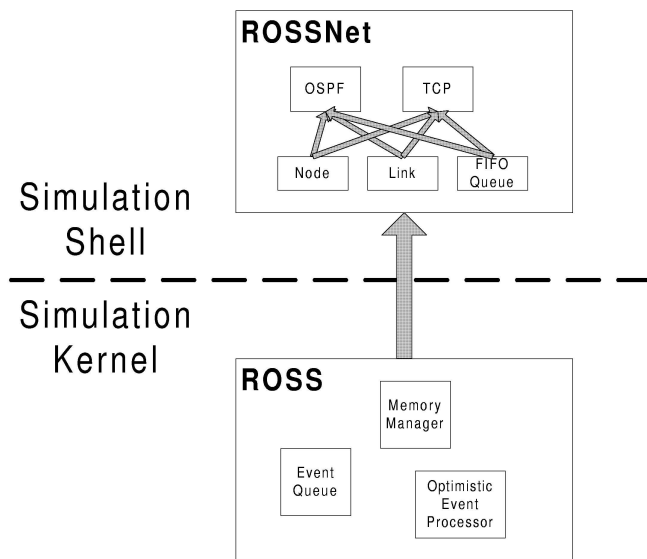


Figure 1: Structure of ROSSNet.

### 3. ROSSNET: TCP MODEL

#### 3.1 TCP Overview

The Internet relies on the TCP/IP protocol suite combined with router mechanisms to perform the necessary traffic management functions. TCP provides reliable transport using a end-to-end window-based control strategy [14]. TCP design is guided by the “end-to-end” principle which suggests that “functions placed at the lower levels may be redundant or of little value when compared to the cost of providing them at the lower level” As a consequence, TCP provides several critical functions, including reliability, congestion control, and session/connection management.

While TCP provides multiplexing/de-multiplexing and error detection using means similar to UDP (e.g., port numbers, checksum), one fundamental difference between them lies is the fact that TCP is connection oriented and reliable. The connection oriented nature of TCP implies that before a host can start sending data to another host, it has to first setup a connection using a 3-way reliable handshaking mechanism.

The functions of reliability and congestion control are coupled in TCP. The reliability process in TCP works as follows:

When TCP sends the segment, it maintains a timer and waits for the receiver to send an acknowledgment on the receipt of the packet. If an acknowledgment is not received at the sender before its timer expires (i.e., a timeout event), the segment is retransmitted. Another way in which TCP can detect losses during transmission is through duplicate acknowledgments, which arise due to the cumulative acknowledgment mechanism of TCP wherein if segments are received out of order, TCP sends a acknowledgment for the next byte of data that it is expecting. Duplicate acknowledgments refer to those segments that re-acknowledge a segment for which the sender has already received an earlier acknowledgment. If the TCP sender receives three duplicate acknowledgments for the same data, it assumes that a packet loss has occurred. In this case the sender now retransmits the missing segment without waiting for its timer

to expire. This mode of loss recovery is called “fast retransmit”.

TCP’s flow and congestion control mechanisms work as follows: TCP uses a window that limits the number of packets in flight, (i.e. unacknowledged). Congestion control works by modulating this window as a function of the congestion that it estimates. TCP starts with a window size of one segment. As the source receives acknowledgments, it increases the window size by one segment per acknowledgment received (“slow start”), until a packet is lost, or the receiver window (flow control) limit is hit. After this event it decreases its window by a multiplicative factor (one half) and uses the variable `ss_thresh` to denote its current estimate of the network bandwidth-delay product. Beyond `ss_thresh` the window size follows a linear increase. This procedure of additive increase/multiplicative decrease (AIMD) allows TCP to operate in an efficient and fair manner [15].

The various flavors of TCP (TCP Tahoe, Reno, SACK) differ primarily in the details of the congestion control algorithms, though TCP SACK also proposes an efficient selective retransmit procedure for reliability. In TCP Tahoe, when a packet is lost, it is detected through the fast retransmit procedure, but the window is set to a value of one and TCP initiates slow start after this. TCP Reno attempts to use the stream of duplicate acknowledgments to infer the correct delivery of future segments, especially for the case of occasional packet loss. It is designed to offer 1/2 round-trip-time (RTT) of quiet time, followed by transmission of new packets until the acknowledgment for the original lost packet arrives. Unfortunately Reno often times out when a burst of packets in a window are lost. TCP NewReno fixes this problem by limiting TCP’s window reduction during a single congestion epoch. TCP SACK enhances NewReno by adding a selective retransmit procedure where the source can pinpoint blocks of missing data at receivers and can optimize its retransmission. All versions of TCP would timeout if the window sizes are small (e.g., small files) and the transfer encounters a packet loss. All versions of TCP implement Jacobson’s RTT estimation algorithm (that sets the timeout to the mean RTT plus four times the mean deviation of RTT, rounded up to the nearest multiple of the timer-granularity (e.g., 500 ms)). A comparative simulation analysis of these versions of TCP was done by Fall and Floyd[16].

#### 3.2 TCP Host Functionality

Our implementation follows the TCP Tahoe specification. Below are the specific capabilities of the ROSSNet TCP session on a single host.

- **Logs:** The system has the ability to log sequence numbers, and congestion control window information. This information was used in our validation study. For performance runs, logging was disabled.
- **Receiver side:** Data is acknowledged when received. If the received packet’s sequence number is NOT equal-to AND is greater-than the expected sequence number, it is stored in the receive buffer. Next, an acknowledgment is sent for the wanted packet (duplicate acknowledgment). When a packet with the expected sequence number is received, the next appropriate acknowledgment is sent according to the receive buffer’s contents.
- **Sender side:** The sender will be in slow-start until the congestion window is greater than the slow-start threshold. After

that, congestion avoidance is started. If three duplicate acknowledgments are observed by the sender, then fast retransmission is performed (see below). If the acknowledgment sequence number is greater than the lowest unacknowledged sequence number, the sender assumes that a gap was filled and sends the appropriate packet.

- **Fast retransmission:** When three duplicate acknowledgments are observed, fast retransmission is started. Here, the slow-start threshold is set to half the minimum congestion window size or the maximum of the receive window. If this value is less than two times the maximum segment size, the slow start threshold is reset to that value. The congestion window is set to maximum segment size.
- **Slow start:** In slow start, two packets are sent for every acknowledgment. Here, the congestion window grows by one maximum segment size every acknowledgment.
- **Congestion avoidance:** The window grows by one maximum segment size every window's worth of acknowledgments. Here, one packet per acknowledgment is normally sent and two packets are sent every congestion window's worth of acknowledgments.
- **Round trip time (RTT):** The RTT is measured one segment at a time. When sending a packet and RTT is not being measured, a new measure is initiated. When retransmitting, cancel the current RTT measurement if ongoing. The RTT measurement process is complete upon receiving the first acknowledgment that covers the RTT packet which is being measured.
- **Round trip timeout (RTO):** We approximate RTO using a weighted average of the past values of RTO and RTT. We are currently implementing Jacobson's tick-based algorithm for computing round trip time, which provides more of a dampen RTO computation by including the deviation its measure [14].

### 3.3 TCP Model Implementation

In the implementation of the TCP model there are three main data structures. The message, which is the data packet, is sent from host to host via the forwarding plane. The router's LP state maintains the queuing information along with the packet loss statistics. Finally the host LP's data structure keeps track of the transferring of data.

A message contains the source and destination address. These addresses are used for forwarding. The message also has the length of the data being transferred which is used to calculate the transfer times at the routers. The acknowledgment number is also included for the sender to observe which packets have been received. The sequence number is another variable which indicates which chunk of data is being transferred.

Now, in our model the actual data transferred is irrelevant and therefore it was not modeled. However in the case that an application was running on top of TCP, such as the Border Gateway Protocol (BGP), packet data is required for the correctness of the simulation. We are currently examining ways in which to optimize this situation as well.

Router state is kept small by exploiting the fact that most of the information is read-only and does not change for the static routing scenarios described in this paper. Inside each router, only queuing information is kept along with a packet loss statistics.

There is a global adjacency list which contains link information. This information is used by the All-Pairs-Shortest-Path algorithm to generate the set of global routing tables (one for each router). Each table is initialized during simulation setup and consists only of the next hop/link number for all routers in the network.

Given the link number, a router can directly lookup the next hop's IP address in its entry of the adjacency list. The adjacency list has an entry for each router and each entry contains all the adjacencies for that router. Along with the router neighbor's address, it contains the speed, buffer size, and link delay for that neighbor.

The host has the same data structures for both the sender and receiver sides of the TCP connection. There is also a global adjacency list for the host, however there is only one adjacency per host. In our model, a host is not multi-homed and can only be connected to one router. There is also a read-only global array which contains the sender or receiver host status, and size of the network transfer. The maximum segment size and the advertised window size were also implemented as global variables to cut down on memory requirements.

The receiver contains a "next expected sequence" variable and a buffer for out-of-order sequence numbers. On the sender side of a connection the following variables are used to complete our TCP model implementation: the round trip timeout (RTO), the measured round trip time (RTT), the sequence number that is being used to measure the RTT, the next sequence number, the unacknowledged packet sequence number, the congestion control window (cnwd), the slow-start threshold, and the duplicate acknowledgment count.

For all experiments reported here, the RTO is initialized to three seconds at the beginning of a transfer, along with the slow start threshold being initialized to 65,536. The maximum congestion window size is set to 32 packets, however this value is easily modified. In addition to the variables needed for TCP, the host has variables for statistics collection. Each host keeps track of the number of packets sent / received, the number of timeouts and its measurement of the transfer's throughput.

Our implementation of the routing table contains only the next hop link number. **Here, the maximum number of links per router is 67. Therefore the routing table could be represented in a byte per entry instead of consuming a full integer size address.** In our simulation we have an entry in the routing table for each router. If we had to have an entry for each host, the routing tables would be extremely large. The hosts were addressed in such a way that the router they are connected to can be inferred and therefore a routing table of only routers is acceptable. In the case that it cannot be inferred, we could have a global table of hosts and the routers that they are connected to. This one table is a lot smaller than having a routing table in each router with every host. We note that some topologies are such that a routing table is not needed, such as a hypercube. In these topologies the next hop can be inferred based on current router and the destination.

Last, we perform a scheduling optimization for routers that implement a drop-tail queuing policy. Here, routers need not keep a queue of packets to be sent. Instead, the routers schedule packets based on the service rate (bytes per seconds) and the timestamp of the last sent packet. As an example, let's assume we have a buffer size of two packets, a service time of 2.0 time units per packet and 4 packets arrive at the following times: 1.0, 2.0, 3.0 and 3.0.

```

ack = SV->unack;
SV->unack = M->ack + g_mss;
/* other operations */
M->ack = ack;

```

**Figure 2: LP state to message data swap example for acknowledgment process.**

```

Forward:

M->dest = SV->cwnd;
SV->cwnd = 1;

Reverse:

SV->cwnd = M->dest;

```

**Figure 3: Swap of the congestion window in a timeout.**

Clearly, the last packet will be dropped, but let's examine how we can implement this without queuing them. If we keep track of the last send time, we see that the packet at 1.0 will be scheduled at 3.0, following 5.0 and 7.0. Thus, when the last packet arrives, the last sent time is 7.0. If we subtract the arrival time of last packet, 3.0 from the last sent time of 7.0, this says there are 4.0 time units worth of data to be sent, which when divided by the service time, yields there are two packets in the queue. Thus, this packet will be dropped. We are currently examining how this approach could be extended to other queuing policies and dynamic routing scenarios. We note here, that other simulation frameworks, such as DaSSF [7], appear to perform this optimization as well.

### 3.4 Reverse Computation

The TCP model uses both reverse computation and incremental state saving. However, as opposed to using a logging structure [17], we reuse data space contained within the event that is currently being processed. This not only reduces the complexity of our simulation engine by not having to perform complex memory management on logs, but also increases data locality. Because we know that the page of memory a message is located will be accessed as a consequence of normal event process, memory overheads (space and time) will not increase by having to swap data between LP state and existing message data.

As an example of how the swap operation is used in our TCP model, consider the processing of an acknowledgment event, as shown in Figure 2. A swap operation is performed between the message's acknowledgment value  $M \rightarrow ack$  and the unacknowledged sequence number contained within the LP's state  $SV \rightarrow unack$ . This is done to effectively state-save the unacknowledged sequence number prior to it being overwritten with new acknowledgment sequence number. The message acknowledgment value can be recreated by subtracting  $g\_mss$  from the unacknowledged sequence number. We also use the message destination to swap the congestion window  $cwnd$  since the packet is already at the destination. Figure 3 shows the forward and reverse code for this swap.

Additionally, we find the receiver's state and the out of order buffer could consume a significant amount of space if copied prior to modification as part of state-saving. The reason for this is because the whole window's worth of packets could be acknowledged with the

```

Forward:

while(SV->out_of_order[cur_var]){
    M->RC.dup_count++;
    SV->out_of_order[cur_var] = 0;
    cur_var++;
}

Reverse:

for(i = M->RC.dup_count; i > 0 ; i--) {
    SV->out_of_order[cur_var] = 1;
    cur_var--;
}

```

**Figure 4: Forward and reverse code for the out-of-order buffer.**

correct sequence number. Thus, the buffer would be completely empty after processing the "acknowledgment" event, resulting in the whole buffer being copied prior to modification.

To avoid this degenerative case, we take a different approach. Here, each buffer entry has a one or a zero depending if the packet is in the buffer. The buffer is circular starting with the next expected sequence number. The only time the buffer changes state dramatically is when a sequence number fills in a gap. The acknowledgment is sent for next missing sequence number. All buffer locations would be set to zero up to the next gap. Because the buffer locations are all consecutive, we are able to count how many were set to zero and record that number as seen in Figure 4. The reverse event handling code uses the packet which was acknowledged and the count to revert the previous values from zero back to one.

## 4. ROSSNET: OSPF MODEL

### 4.1 OSPF Overview

Routing protocols in the Internet could be classified into two main groups: *link-state routing* and *distance-vector routing*. Typically in the current Internet, distance-vector routing protocols (e.g., BGP) are used for inter-domain routing (i.e., routing among Autonomous Systems (ASs)), while link-state routing protocols (e.g., OSPF, and IS-IS) are used for intra-domain routing. As all the other link-state routing protocols, OSPF maintains a *map* of the network (which typically corresponds to one AS in the Internet) at all routers. Each router collects their local link information and floods the network with that information so that all the routers have a global map of the network.

In OSPF, routers send HELLO packets to their neighbors to check whether they are up or down. HELLO packets are sent periodically at every HelloInterval. If the neighbor does not respond after some period of time, then it is assumed dead. This period of time is called the RouterDeadInterval, and is typically four times the HelloInterval.

Each router maintains link status announcements (LSAs) received from other routers. Collection of these LSAs is called a Link-State Database (LS-Database), which in fact shows the global map of the network. The routers run Dijkstra's or some other shortest path algorithm to find the routes in the network. When a link goes down or comes up, the routers detect the change via HELLO messages.

After updating its local LS-Database, the router send an LS-Update message which conveys the change to other routers. Normally, LS-Update messages are sent when a change in the LS-Database occurs. Such a change can happen either because of a local link, or because of an LS-Update message received from elsewhere. There is also LS-Refresh messages sent across the OSPF routers. Each OSPF router floods its LS-Database to other routers at every LSRefreshInterval, which is typically 45 minutes.

For scalability purposes, OSPF divides an AS into areas and constructs a hierarchical routing among the areas. For each area, a corresponding Area Border Router (ABR) is assigned. In addition to ABRs, there are Backbone Routers which are the router nodes among which inter-area routing takes place. Among ABRs and Backbone Routers, one router is assigned as the Boundary Router, which is responsible for routing to/from other ASs. All these assignments of routers are typically done manually in the current Internet. Multi-area routing in OSPF helps scalability. LSAs are flooded only in the area, rather than the whole AS. ABRs flood internal LSAs to other areas as Summary-LSAs. This scales flooding of LSAs. Also, routing among Backbone Routers occurs based on address prefixes, which scales routing tables.

## 4.2 OSPF Model Implementation

The OSPF messages can become fairly large (for example, database description packet-exchange and subsequent LS Updates in response to the LS Requests). These long messages can be a big impediment to model scalability. In order to keep messages as small as possible, we use pointers to a message, instead of the actual large message data structure. Under this approach, the router which creates the message, allocates the memory and fills in the required information, and just sends across the pointer. Depending upon the type of message, the memory allocated is freed by the entity receiving the message or the entity originating the message.

In the OSPF model, HELLO messages appear to take the largest share of total event/message population. Typically, there is one event to wake up the interface after every HELLO Interval, and then one event to send the actual HELLO message. This means that two events are required to generate one HELLO message. In our model, we schedule just one event to wake up the router, and then the router sends the HELLO messages with some randomization out of every interface. This significantly reduces the number of events in the simulation.

The LS-Database consumes up the largest share of memory, which is stored on every router. This is the biggest limitation to scalability (in terms of number of routers) of an OSPF simulation model. The information required to compare two LSAs, when an LS-Update is received, is stored in the LS-Header. In practice, the link information is replicated at every router and in every LSA. We simulate this by storing only one Link Information Table (LIT) that includes one copy of each link in the topology. So, in our simulation, we store only one copy of the link information (for each link in the topology) globally as shared among all the routers, instead of having a redundant separate copy for each. We store the LS-Headers locally at each router, so that routers are able to individually age the LSAs and refresh the self-generated LSAs periodically.

In the case of a link outage, the router connected to that link detects the change, and schedules an LS-Update, which consists of the new LS-Header. In the simulation, we reflect this link outage by updating the LIT. Routers receiving the LS-Update can use the

LIT to run the shortest-path algorithm, and calculate its forwarding table. This method works well for a single link outage before the network converges. However, a problem with the above strategy arises when there are multiple and frequent link outages or recoveries in the simulated scenario. Here, nodes in the network will observe different states of the network depending on the arrival order of LS-Updates. For example, assume there are two subsequent link outages that happened for links A and B. It will such that some nodes will hear outage of link A earlier than outage of link B, and some other nodes will hear the other way around. So, if there are multiple link changes within one convergence time, then ways of handling the situation in the model are more complicated.

One possible method of solving this problem is to use multiple copies of the LIT, each for one possible arrival order of LS-Update messages. In this approach, the recipient of LS-Update message selects which copy of the LIT to use based on the previous LS-Update messages it has received. One fundamental problem with this approach, is that the size of LIT is enormous for a network with millions of nodes and links. So, each copy is a significant burden in terms of memory consumption, which is the main bottleneck for simulation scalability.

Finally, we note here that our OSPF model lacks the reverse execution code path to support optimistic parallel execution. That functionality will be available in the very near future. Consequently, all our OSPF results are based on sequential model execution.

## 5. EXPERIMENTAL VALIDATIONS

In this section we will present simple simulation scenarios where we can demonstrate that our implementations of TCP and OSPF protocols are valid and accurate. In order to validate our TCP implementation, we show the matching between our TCP implementation and SSFNet's TCP implementation. To validate our OSPF implementation, we run our OSPF implementation on a four-router network and observe changes in the forwarding tables as some of the links are taken down or up.

### 5.1 TCP Validation

SSFNet [6] has a set of validation test which shows the basic behavior of TCP. Because of space limitations, we only show how ROSSNet's TCP compares with SSFNet for the Tahoe fast retransmission timeout behavior. This test is configured with a server and a client TCP session with a router in between. The bandwidth is 8 Mb/sec from the server to the router with 5 ms delay and the client to the router had a bandwidth of 800 kilobit per second with a 100 ms delay. The server was transferring a file of 13,000 bytes.

As can be seen from Figures 5-a and 5-b, our implementation with respect sequence number and congestion window behavior performs very similar. The packet drop happens at similar times and so does the fast retransmission.

### 5.2 OSPF Validation

In order to validate our OSPF simulation, we experiment on a small topology as shown in Figure 6. There are four routers numbered from 0 to 3, and four end-nodes numbered from 4 to 7. Routers are shown as gray nodes in the Figure 6. Links among the routers are all 10 Mb, while the links connecting routers to end-nodes are all 1 Mb in capacity. In Figure 6, numbers written on each link represents the OSPF weight (or cost) for that link. Also, numbers that are written at the beginning of each arrow represents the local enu-

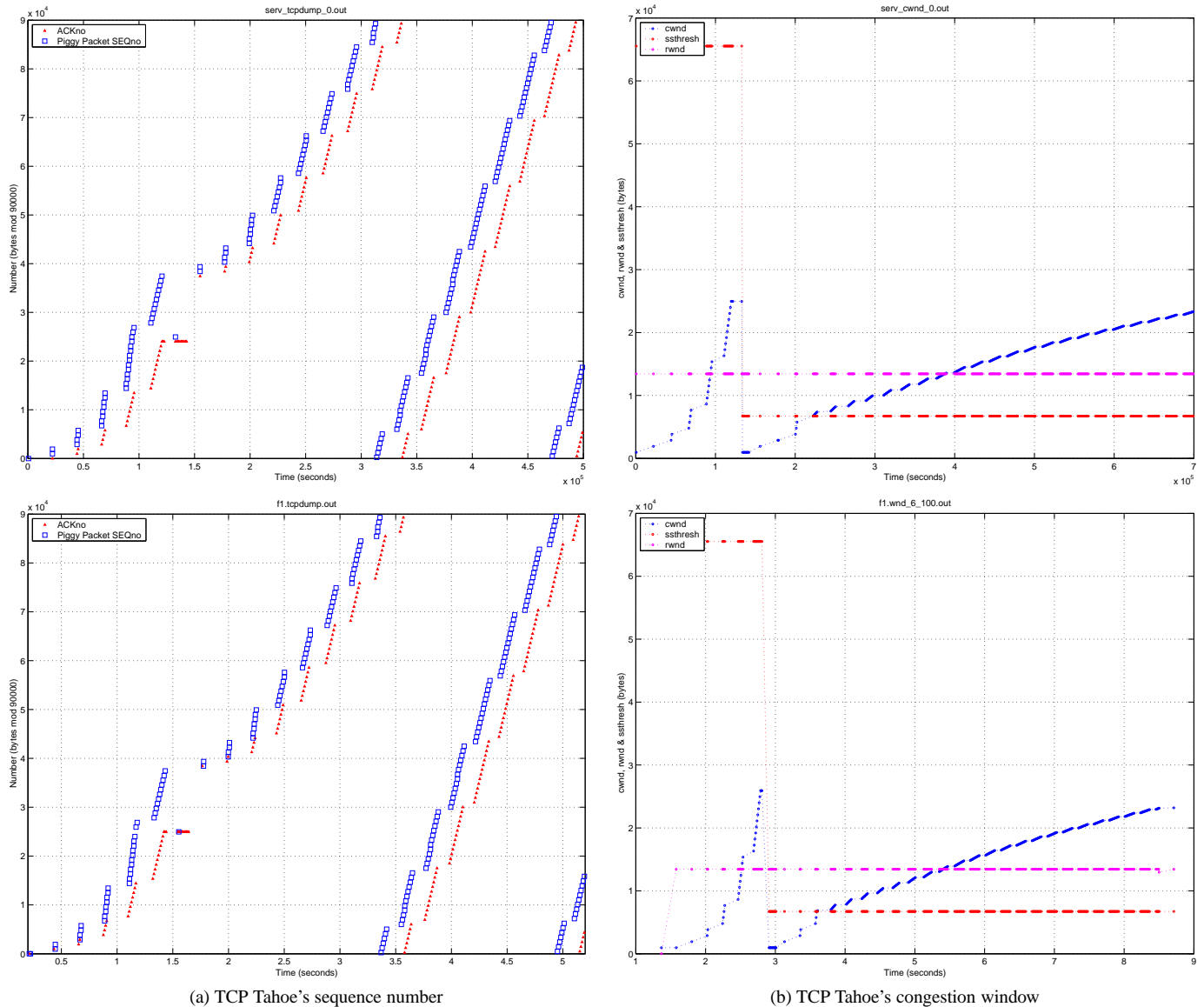


**Figure 5: Comparison of SSFNet and ROSSNet TCP models based on (a) sequence number, (b) congestion window for TCP Tahoe fast retransmission behavior. Top panel is ROSSNet and bottom panel is SSFNet.**

meration of the link at that node. These enumerations are necessary for forwarding of the packets.

We simulated a scenario where there are two TCP flows. One of the TCP flows starts at node 4 and ends at node 7. The other TCP flow starts at node 5 and ends at node 6. The TCP flows were run for a total simulation time of 500 seconds. At time 50, the bi-directional link (i.e., the two one-way links) in between routers 0 and 2 goes down. Later at time 250, it comes back up. We observed the routing tables at the routers and behavior of the two TCP flows.

Table 1 shows the observed routing tables at the four router nodes during the three stages of the simulation. Please note, we did not include entries for end-nodes for simplification. A 255 means the next node is “self”. Observe that router nodes correctly adjust themselves in response to the two link changes. There is also no

change in the behavior of TCP flows, because their routes remain the same and are not affected by the link changes.

## 6. PERFORMANCE RESULTS

### 6.1 Configuration

Our experiments were conducted on a dual Hyper-Threaded Pentium-4 Xeon processor system running at 2.8 GHz. *Hyper-Threading* is Intel’s name for a simultaneous multithreaded (SMT) architecture [18]. SMT supports the co-scheduling of many threads or processes to fill-up unused instruction slots in the pipeline caused by control or data hazards. Because the system knows that there can be no control or data hazards between threads, all threads or processes that are ready to execute can be simultaneously scheduled. In the case of threads that share data, mutual exclusion is guarded by locks. Consequently, the underlying architecture need not know

**Table 1: Routing tables for three stages of the simulation for OSPF validation.**

Simulation Stage	Router 0		Router 1		Router 2		Router 3	
	Desti- nation	Next Node	Desti- nation	Next Node	Desti- nation	Next Node	Desti- nation	Next Node
0-50	0	<b>255</b>	0	0	0	<b>2</b>	0	1
	1	<b>0</b>	1	255	1	<b>0</b>	1	0
	2	<b>2</b>	2	1	2	<b>255</b>	2	0
	3	<b>1</b>	3	0	3	<b>1</b>	3	255
50-250	0	<b>255</b>	0	0	0	<b>0</b>	0	1
	1	<b>0</b>	1	255	1	<b>0</b>	1	0
	2	<b>1</b>	2	1	2	<b>255</b>	2	0
	3	<b>1</b>	3	0	3	<b>1</b>	3	255
250-500	0	<b>255</b>	0	0	0	<b>2</b>	0	1
	1	<b>0</b>	1	255	1	<b>0</b>	1	0
	2	<b>2</b>	2	1	2	<b>255</b>	2	0
	3	<b>1</b>	3	0	3	<b>1</b>	3	255

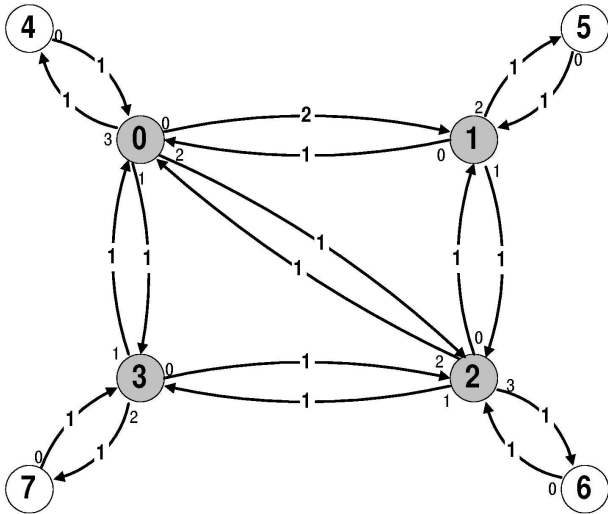


**Figure 6: Topology for experimental validation of OSPF simulation.**

about shared variables or how they are used at the program level. Additionally, because the threads assigned to the same physical processor share the same cache, there is no additional hardware needed to support a cache-coherency mechanism.

Intel's Hyper-Threaded architecture supports two instruction streams per processor core [19]. From the OS scheduling point-of-view, each physical processor appears as if there are two distinct processors. Under this mode of operation, an application must be threaded to take advantage of the additional instruction streams. The dual-processor configuration behaves as if it was a quad processor system. Because of multiple instruction streams per processor, we denote instruction stream (IS) count instead of processor count in our performance study to avoid confusing the issue between physical processor counts and virtual processors or separate instruction streams.

The total amount of physical RAM is 6 GB. The operating system is Linux, version 2.4.18 configured with the 64 GB RAM patch. Here, each process or group of threads (globally sharing data) is limited to a 32 bit address space, where the upper 1 GB is reserved for the Linux kernel. Thus, an application is limited to 3 GBs for all code and data (both heap and stack space and thread control data structures).

For all experiments, each TCP connection used a uniform configuration. The transfer size was infinite, allowing the transfers to run for the duration of the simulation. The maximum segment size was set to 960 bytes. The total size of all headers was 40 bytes. The initial sequence number was initialized to zero and the slow start threshold was 65,536.

All clients and servers were connected in the way that the first half of hosts randomly connected to the second half of hosts. There was a distinct client-server pair for each TCP connection in the simulation. Because of the random nature of connections, there was a high percentage of "long-haul" links that result in a large number of remote events scheduled between processors / instruction streams.

**Table 2: Performance results for  $N = 4, 8, 16, 32$  synthetic topology network for low (500 Kb), medium (1.5 Mb) and high (45 Mb) bandwidth scenarios on 1, 2 and 4 instruction streams using a dual Hyper-Threaded 2.8 GHz Pentium-4 Xeon. Efficiency is the net events processed (i.e., excludes rolled back events) divided by the total number of events. Remote is the percentage of the total events processed sent between LPs mapped to different threads/instruction streams.**

Number of Nodes, $N$	End Host Bandwidth	Num IS	Event Rate	Efficiency	% Remote	Speedup
4	500 Kb	1	441692	NA	NA	NA
4	500 Kb	2	535093	<b>99.388</b>	7.273	1.211
4	500 Kb	4	660693	<b>97.411</b>	14.308	1.495
4	1.5 Mb	1	386416	NA	NA	NA
4	1.5 Mb	2	440591	<b>99.972</b>	7.125	1.140
4	1.5 Mb	4	585270	<b>99.408</b>	14.195	1.516
4	45 Mb	1	402734	NA	NA	NA
4	45 Mb	2	440802	<b>99.445</b>	7.087	1.094
4	45 Mb	4	586010	<b>99.508</b>	14.312	1.612
8	500 Kb	1	210338	NA	NA	NA
8	500 Kb	2	270249	<b>100</b>	7.273	1.284
8	500 Kb	4	331451	<b>99.793</b>	10.746	1.575
8	1.5 Mb	1	177311	NA	NA	NA
8	1.5 Mb	2	237496	<b>100</b>	7.313	1.339
8	1.5 Mb	4	287240	<b>99.993</b>	10.823	1.619
8	45 Mb	1	176405	NA	NA	NA
8	45 Mb	2	221182	<b>99.999</b>	7.259	1.253
8	45 Mb	4	257677	<b>99.996</b>	10.758	1.460
16	500 Kb	1	128509	NA	NA	NA
16	500 Kb	2	172542	<b>100</b>	7.091	1.342
16	500 Kb	4	199282	<b>99.987</b>	10.600	1.550
16	1.5 Mb	1	100980	NA	NA	NA
16	1.5 Mb	2	137493	<b>100</b>	7.092	1.361
16	1.5 Mb	4	153454	<b>99.998</b>	10.626	1.519
16	45 Mb	1	99162	NA	NA	NA
16	45 Mb	2	117312	<b>100</b>	7.102	1.183
16	45 Mb	4	145628	<b>99.999</b>	10.648	1.468
32	500 Kb	1	80210	NA	NA	NA
32	500 Kb	2	108592	<b>100</b>	7.058	1.353
32	500 Kb	4	126284	<b>100</b>	10.586	1.57
32	1.5 Mb	1	75733	NA	NA	NA
32	1.5 Mb	2	90526	<b>100</b>	7.052	1.20

**Table 3: Memory requirements for  $N = 4, 8, 16, 32$  synthetic topology network for low (500 Kb), medium (1.5 Mb) and high (45 Mb) bandwidth scenarios on 1, 2 and 4 instruction streams using a dual Hyper-Threaded 2.8 GHz Pentium-4 Xeon. Optimistic processing only required 7000 more event buffers (140 bytes each) on average which is less 1 MB.**

Number of Nodes, $N$	Host Bandwidth	Max Event-list Size	Memory Requirements
4	500 Kb	4,792	<b>3 MB</b>
4	1.5 Mb	5,376	<b>3 MB</b>
4	45 Mb	5,376	<b>3 MB</b>
8	500 Kb	45,759	<b>11 MB</b>
8	1.5 Mb	85,685	<b>17 MB</b>
8	45 Mb	86,016	<b>17 MB</b>
16	500 Kb	522,335	<b>102 MB</b>
16	1.5 Mb	1,217,929	<b>202 MB</b>
16	45 Mb	1,380,021	<b>226 MB</b>
32	500 Kb	5,273,847	<b>1,132 MB</b>
32	1.5 Mb	6,876,362	<b>1,364 MB</b>

Last, ROSS is configured with a binary heap for all TCP experiments. However, we have recently implemented a Splay Tree for event-list management and find it produces a 50 to 100% performance improvement over the binary heap. All OSPF experiments have ROSS configured with the faster performing Splay Tree.

## 6.2 Synthetic Topology Experiments

The synthetic topology is fully connected at the top and has four levels. A router at one level is connected to  $N$  lower level routers or hosts. The total number of nodes is equal to  $N^4 + N^3 + N^2 + N$ .  $N$  was varied between, 4, 8, 16, and 32. The nodes are numbered in such a way that the next hop can be calculated based on the destination at each hop.

The bandwidth, delay and buffer size for the synthetic topology is as follows:

- 2.48 Gb/sec, a delay of 30 ms, and 3 MB buffer,
- 620 Mb/sec, a delay between 10 ms to 30 ms, and 750 KB buffer,
- 155 Mb/sec, a delay of 5 ms, 10ms and 30ms, and 200 KB buffer,
- 45 Mb/sec, a delay of 5 ms, and 60 KB buffer,
- 1.5 Mb/sec, a delay of 5 ms, and 20 KB buffer,
- 500 Kb per second, a delay of 5 ms, and 15 KB buffer

We consider three bandwidth scenarios: (i) *high*, which has 2.48 Gb/sec for the top-level router link bandwidths, and each lower level in the network topology uses the next lower bandwidth shown above yielding a host bandwidth of 45 Mb/sec, (ii) *medium*, which starts with 620 Mb/sec and goes down to 1.5 Mb/sec at the end host, and (iii) *low*, which starts with 155 Mb/sec and goes down to 500 Kb/sec at the end host. These bandwidths and link delays are realistic relative to networks in practice [20]. We provide more information about the AT&T topology below in Section 6.3.

Our experiments were run on 1, 2 and 4 instructions streams (IS). The synthetic topology is mapped with each core router and all its children assigned to the same processor.

Table 2 shows the performance results for all synthetic topology scenarios across varying numbers of available instruction streams on the Hyper-Threaded system. For all configurations, we report an extremely high degree of efficiency, as shown in the highlighted column. The lowest efficiency is 97.4% and to our surprise we observe a large number of zero rollback cases for 2 and 4 instruction streams resulting in 100% simulator efficiency. We observe that the amount of available work per instruction stream (IS) retards the rate of forward progress of the simulation, particularly as  $N$  grows and the bandwidth increases. Thus, remote messages arrive ahead of when they need to be processed resulting in almost perfect simulator efficiency. This result holds despite an inherently small lookahead which is a consequence of link delay (ranging between 5 to 30 ms) and a large amount of remote events (ranging between 7% to 15%).

The observed speedup ranges between 1.2 and 1.6 on the dual-hyper-threaded processor system. These speedups are very much

in line with what one would expect, particularly given the memory size of the models at hand relative to the small level-2 cache. We note that we were unable to execute the  $N = 32$ , 45 Mb bandwidth case. This aspect and memory overheads are discussed in the paragraphs below.

The memory footprint of each model is shown as a function of nodes and bandwidth in Table 3. We report a steady increase in memory requirements and event-list size as bandwidth and the number of nodes in the network increase. The peak memory usage is almost 1.4 GB of RAM for the  $N = 32$ , 1.5 Mb bandwidth scenario. The amount of additional memory allocated for optimistic processing is 7000 event buffers which is less than 1 MB. Thus, for 524288 TCP connections, this model only consumes 2.6 KB per connection including event data. By comparison, Nicol [21] reports that Ns consumes 93 KB per connection, SSFNet (Java version) consumes 53 KB, JavaSim consumes 22 KB per connection and SSFNet (C++ version) consumes 18 KB for the “dumbbell” model which contains only two routers.

Last, we find that there is an interplay in how the event population is effected by the network size, topology, bandwidth and buffer space. In examining the memory utilization results, we find that the maximum observed event population differs by only a moderate amount for 1.5 Mb versus 45 Mb case when  $N = 16$  despite a rather significant change in network buffer capacity. However, we were unable to execute the 45 Mb scenario when  $N = 32$  because it requires more than 17,000,000 events, which is the maximum we can allocate for that scenario without exceeding operating system limits ( $\sim 3$  GB of RAM). This is because there are many more hosts at a high bandwidth, resulting in much more of the available buffer capacity to be occupied with packets waiting for service. This case results in a 2.5 times increase in the amount of required memory. This suggested, model designers will have to perform some capacity analysis, since networks memory requirements may explode after passing some size, bandwidth or buffer capacity threshold, as happened here.

### 6.2.1 Hyper-Threaded vs. Multiprocessor System

In this series of experiments we compare a standard quad processor system to our dual, hyper-threaded system in order to better quantify our performance results relative to past processor technology. The network topology is the same as previously described with  $N = 8$ , thus there are 4680 LPs in this simulation. We did however modify the TCP connections such that they are more locally centered. In total 87% of all TCP connections were within the same kernel process (KP).

We observe that the dual processor out performs the quad processor system by 16% despite that the quad processor having two times the amount of level-2 cache (each quad processor has 512 KB for a total of 2 MB of cache). The respective speedups relative to their own sequential performance are 3.2 for the quad processor and 1.7 for the dual hyper-threaded system, which is 80 to 85% of the theoretical maximum. If we compare cost-performance, the dual hyper-threaded system ( $\sim$ \$7000 USD) is the clear winner over the quad processor system ( $\sim$ \$24,000 USD) by over a factor of three, since it costs less than 1/3 the price at the date of purchase.

Additionally, we observe 100% simulator efficiency for all parallel runs. We attribute this phenomenon to the low remote messages and large amount of work (event population) per unit of simulation time.

**Table 4: Performance results for  $N = 8$  synthetic topology network medium bandwidth on 1, 2 and 4 instruction streams (dual Hyper-Threaded 2.8 GHz Pentium-4 Xeon) vs. 1, 2 and 4 processors (quad, 500 MHz Pentium-III).**

Processor Configuration	Event Rate	% Efficiency	% Remote	Speedup
1 IS, Hyper-Threaded	220098	NA	NA	NA
2 IS, Hyper-Threaded	313167	<b>100</b>	0.05	1.42
4 IS, Hyper-Threaded	375850	<b>100</b>	0.05	1.71
1 PE, Pentium-III	101333	NA	NA	NA
2 PE, Pentium-III	183778	<b>100</b>	0.05	1.81
4 PE, Pentium-III	324434	<b>100</b>	0.05	3.20

### 6.3 AT&T Topology Experiments

For our performance study we used AT&T’s network topology obtained from the Rocketfuel Internet topology database [22].

As shown in Figure 7, the core US AT&T network topology contains 13173 router nodes and 38164 links. What makes Internet topologies like the AT&T network both interesting and challenging from a modeling prospective is its sparse connectivity and power-law structure [22]. In the case of AT&T, there are less than 3 links per router on average. However, at the super core there is a high-degree connectivity. Typically, an Internet service provider’s super core will be configured as a fully connected mesh. Consequently, backbone routers will have up to 67 connections to other routers, some of which are other backbone or super core routers and other links to region core routers. Once at the region core level, the number of links per router reduces and thus the connectivity between other region cores is sparse. Most of the connectivity is dedicated to connecting local points of presence (PoPs).

In performing a breadth-first-search of the AT&T topology, there are distinct eight levels. At the backbone, there are 414 routers. At each successive level yields the following router count : 4861, 5021, 1117, 118, 58, 6 and at the final level there are 5 nodes. There were a number of routers not directly reachable from within this network. Those routers are most likely transit routers going strictly between autonomous systems (AS). With the transit routers removed, our AT&T network scenario has 11670 routers. Link weights are derived based on the relative bandwidth of the link in comparison to other available links. In this configuration, routing is keep static.

The bandwidth, delay, and buffer size for the AT&T topology is as follows:

- *Level 0 router:* 9.92 Gb/sec, a delay randomly between 10 ms to 30 ms, and 12.4 MB buffer.
- *Level 1 router:* 2.48 Gb/sec, a delay randomly between 10 ms to 30 ms, and 3 MB buffer.
- *Level 2 router:* 620 Mb/sec, a delay randomly between 10 ms to 30 ms, and 750 KB buffer.
- *Level 3 router:* 155 Mb per second, a delay of 5 ms, and 200 KB buffer.
- *Level 4 router:* 45 Mb per second, a delay of 5 ms, and 60 KB buffer.
- *Level 5 router:* 1.5 Mb/sec, a delay of 5 ms, and 20 KB buffer.

- *Level 6 router:* 1.5 Mb per second, a delay of 5 ms, and 20 KB buffer.
- *Level 7 router:* 500 Kb per second, a delay of 5 ms, and 5 KB buffer.
- *link to all hosts:* 70 Kb per second, a delay of 5 ms, and 5 KB buffer.

Hosts are connected in the network at PoP level routers. These routers only have one link to another higher-level router.

The first configuration is medium size, with 96,500 nodes or LPs (hosts plus routers) total, and the second is large, with 266160 LPs. In each configuration, one half the host population establishes a TCP session to a *randomly selected* receiving host. *We observe this configuration is almost pathological for a parallel network simulation because the amount of remote network traffic will be much greater than is typical in practice.* The amount of remote message traffic is much greater than the synthetic network topology because of the network’s sparse structure. Our goal is to demonstrate simulator efficiency under high-stress workloads for realistic topologies.

We observe over 99% efficiency for the 2 and 4 IS runs as shown in Table 5, yet there is a substantial reduction in the overall obtain speedup. Here, we report speedups for the 4 IS cases of 1.25 for the medium size network and 1.29 for the large. We attribute this reduction to enormous amount of remote messages sent between instruction streams/processors. A parallel simulation using the AT&T network topology with a round-robin mapping of LP to processors results 50 to 80% of the all processed events being remotely schedule. We hypothesize that these high remote message rates reduce memory locality and results in much higher cache miss rates. Consequently, all instruction streams are spending more time stalled waiting for memory requests to be satisfied.

The memory requirements for the AT&T scenario were 269 MB for the medium size network and 328 MB for the large size network, yielding a per TCP connection overhead of 2.8 KB and 1.3 KP respectively. The reason for the reduction per connection in moving from medium to large configuration is because the amount of network buffer space which effects the peak event population did not change, yet the number of connections went up by almost a factor of three.

### 6.4 Initial OSPF Results

Our OSPF experiments use the same AT&T topology configuration as described for the medium network size (i.e., 96,500 nodes total in the network). However, we do increase the bandwidth for levels

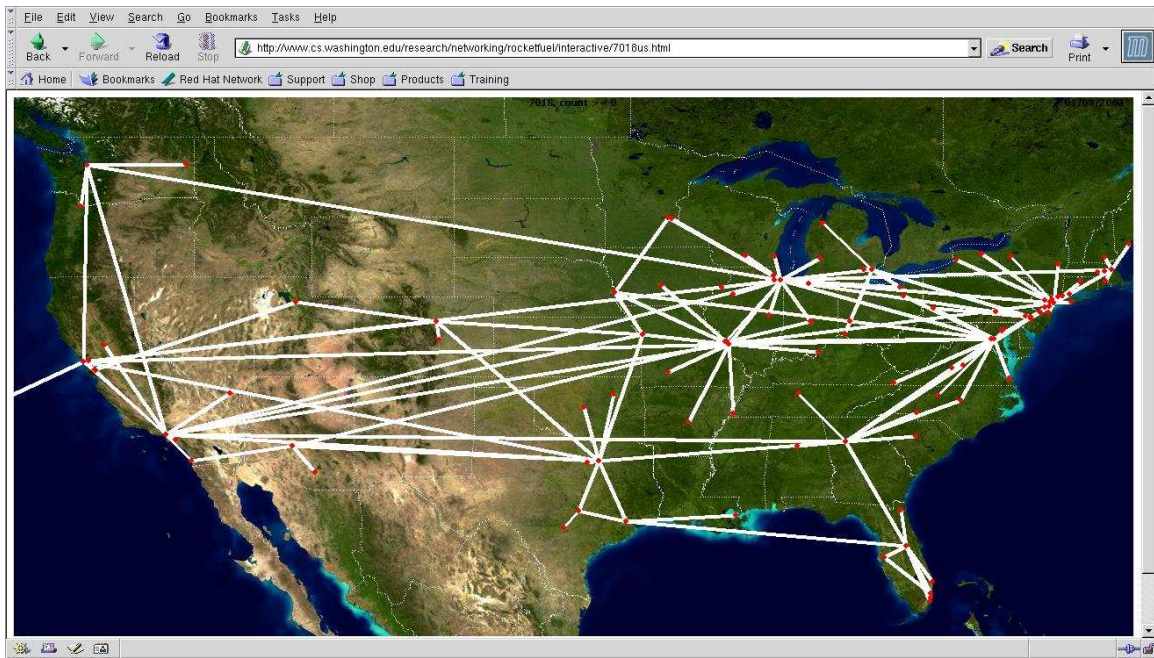


Figure 7: AT&T Network Topology (AS 7118) from the Rocketfuel data bank for the continental US.

Table 5: Performance results for AT&T network topology for medium (96,500 LPs) and large (266160) on 1, 2 and 4 instruction streams (IS) using the dual-hyper-threaded system.

Configuration	Event Rate	% Efficiency	% Remote	Speedup
medium, 1 IS	138546	NA	NA	NA
medium, 2 IS	154989	<b>99.947</b>	52.030	1.12
medium, 4 IS	174400	<b>99.005</b>	78.205	1.25
large, 1 IS	127772	NA	NA	NA
large, 2 IS	143417	<b>99.956</b>	51.976	1.12
large, 4 IS	165197	<b>99.697</b>	78.008	1.29

Table 6: OSPF with TCP Performance results for AT&T topology (96,500 LPs) scenarios on 1 instruction stream using a dual Hyper-Threaded 2.8 GHz Pentium-4 Xeon. Simulates 100 seconds of network traffic.

Configuration	Event Rate	Max Event-list Size	Events Processed	Memory Requirements
OSPF, no TCP	419286.66	150000	796200468	<b>1.92 GB</b>
OSPF with TCP	197954.02	1800000	1783473402	<b>2.29 GB</b>

5, 6 and 7 to 45 Mb/sec. Thus, the amount of traffic generated by the TCP hosts is much greater in this scenario. We also note that we configure all routers in the AT&T network to be inside a *single* OSPF area. Consequently, this results in extremely large OSPF routing tables (i.e.,  $N^2$  for  $N$  routers in an area) and we are in effect simulating a pathological OSPF scenario as the typical “rule of thumb” for OSPF limits the number of routers per area to 50 [23] with an operational upper bound between 200 to 1000 even with an optimized router. *Our area is 12 to 200 times those design limits.* However, despite these modeling extremes we are able to simulate this scenario in conjunction with TCP background traffic, as shown in our performance results (see Table 6).

As shown in Table 6, we observe that the event rate is kept high by

the Splay Tree for OSPF without TCP flows, however as we add TCP flows the event population increases by a factor of 12 (150K to 1.8 M). With this increase, the event-list management overheads rise by a factor of two which results in a sharp decrease in the event rate.

The memory utilization is quite large for our models, ranging from 1.9 to 2.3 GB of RAM. We attribute high memory usage to the size of the adjacency matrix and routing tables. Recall, this model configures OSPF as a single area. While our state compression techniques do in fact reduce memory consumption, this pathological runtime configuration still requires substantial memory requirements. In practice, we anticipate much smaller tables for multi-area OSPF scenarios and significantly less memory.

## 7. RELATED WORK

Much of the current research in parallel simulation for network models is largely based on conservative algorithms. PDNS [8] is parallel/distributed network simulator that leverages HLA-like technology to create a federation of Ns [5] simulators. SSFNet [6], TasKit[24] and GloMoSim [25] all use Critical Channel Traversing (CCT) [24] as the primary synchronization mechanism. DaSSF employs a hybrid technique called *Composite Synchronization*[7], where both the asynchronous CCT algorithm and a barrier synchronization are combined to avoid channel scanning limitations associated CCT while at the same time reducing the frequency a global barrier must be applied.

Recent optimistic simulation systems for network models include TeD [26], which is a process-oriented framework for constructing high-fidelity telecommunication system models. Premore and Nicol [27] implement a TCP model in TeD, however no performance results are given. USSF [12] is an optimistic simulation system that dramatically reduces model run-time state by LP aggregation, and swapping LPs out of core. Additionally, USSF proposes to execute simulations unsynchronized using their NOTIME approach. Based on the results here, a NOTIME synchronization could prove beneficial for large-scale TCP models. Unger et. al. simulate a large-scale ATM network using an optimistic approach [28]. They report speed-ups ranging from 2 to 7 on 16 processors and indicate that optimistic outperforms a conservative protocol on 5 of the 7 tested ATM network scenarios. Finally, a new fixed-point optimistic approach, called Genesis has been proposed by Szymanski et. al.[29]. This approach yields speedups up to 18 on 16 processors for 64 to 256 node TCP models. Super-linear performance is attributed to a reduction in the number of events schedule across machines because of the statistical aggregation of events which is employed by this approach.

## 8. CONCLUSIONS AND DISCUSSIONS

In this paper, we propose solutions for the problem of scaling network simulations to millions of nodes. Based on the proposed techniques, we develop scalable simulation models for the OSPF routing protocol and TCP transport protocol. We ran simulations of these models on a very large and realistic topology. To date, this capability has not been demonstrated.

With the use of optimistic parallel simulation techniques coupled with reverse computation, speedups of 1.7 for a hyper-threaded dual processor system and 3.2 for a quad processor system are reported. These speedups were achieved with an insignificant amount of additional memory for optimistic processing (i.e.,  $\approx 1$  megabyte in practice).

The parallel TCP model proved to be extremely efficient with very few rollbacks observed. Parallel simulator efficiency ranged between 97 to 100% (i.e., zero rollbacks). This suggests that the model could be executed *unsynchronized* with a negligible amount of error.

The model was implemented as lean as possible which allowed for the million node topology to be executed on an inexpensive COTS multiprocessor system. We observed model memory requirements between 1.3 KB to 2.8 KB per TCP connection depending on the network configuration (size, topology, bandwidth and buffer capacity).

The hyper-threaded system was able to provide a low cost / per-

formance ratio. What is even more interesting is that these systems blur the lines in terms of sequential versus parallel processing. Here, to obtain higher rates of performance from a single processor, one has to resort to executing the model in parallel. As this technology matures to even high clock rates, we anticipate single processors having many more instruction streams, which will provide an even greater opportunity for parallel simulation tools and techniques.

There have been many ideas that have come about during this work. In the future, we plan to develop a scalable simulation model for BGP and investigate inter-domain routing issues. We will also be working on the implementation for a faster event-list management algorithm to reduce priority queue overheads. Also the implementation of TCP functionality such as delayed acknowledgments, ticks for round trip time calculation, and Reno capabilities are work in progress. The concept of creating a hierarchical address mapping scheme from a random network topology as well as a better LP to processor mapping scheme to reduce remote events is also being examined.

Finally, in the creation of these models, we leveraged existing models in both the Ns-2 and SSFNet frameworks. We find that “porting” model functionality to our platform is relatively straight forward. In the future, we plan to devise porting guidelines and provide detailed case studies of how we have ported OSPF, TCP, and BGP for use as a reference.

## 9. REFERENCES

- [1] E.G. Coffman, Z. Ge, V. Misra, and D. Towsley, “Network resilience: Exploring cascading failures within bgp,” in *Proceedings of the 40th annual Allerton Conference on Communications, Computing and Control*, 2002.
- [2] A. Shaikh, L. Kalampoukas, R. Dube, and A. Varma, “Routing stability in congested networks: Experimentation and analysis,” in *Proceedings of ACM Conference on Applications, Technologies, Architectures, and Protocols for Computer Communications (SIGCOMM)*, 2000.
- [3] D. R. Jefferson, “Virtual time,” *ACM Transactions on Programming Languages and Systems*, vol. 7, no. 3, pp. 404–425, July 1985.
- [4] C. D. Carothers, K. Perumalla, and R. M. Fujimoto, “Efficient parallel simulation using reverse computation,” *ACM Transactions on Modeling and Computer Simulation*, vol. 9, no. 3, pp. 224–253, July 1999.
- [5] “UCB/LBLN/VINT network simulator - ns (version 2),” <http://www-mash.cs.berkeley.edu/ns>, 1997.
- [6] J. Cowie, H. Liu, J. Liu, D. Nicol, and A. Ogielski, “Towards realistic million-node internet simulations,” in *Proceedings of International Conference on Parallel and Distributed Processing Techniques and Applications (PDPTA)*, 1999.
- [7] D. M. Nicol and J. Liu, “Composite synchronization in parallel discrete-event simulation,” *IEEE Transactions on Parallel and Distributed Systems*, vol. 13, no. 5, 2002.
- [8] G. F. Riley, R. M. Fujimoto, and M. H. Ammar, “A generic framework for parallelization of network simulations,” in *Proceedings of the 7th International Symposium on Modeling, Analysis and Simulation of Computer and*

- Telecommunication Systems (MASCOTS)*, 1999, pp. 128–135.
- [9] P. L'Ecuyer and T. H. Andres, "A random number generator based on the four lcms," *Mathematics and Computers in Simulation*, vol. 44, pp. 99–107, 1997.
- [10] R. Brown, "Calendar queues: A fast  $o(1)$  priority queue implementation for the simulation event set problem," *Communications of the ACM (CACM)*, vol. 31, pp. 1220–1227, 1988.
- [11] R. Ronngren and Rassul Ayani, "A comparative study of parallel and sequential priority queue algorithms," *ACM Transactions on Modeling and Computer Simulation*, vol. 7, no. 2, pp. 157–209, April 1997.
- [12] D. M. Rao and P. A. Wilsey, "An ultra-large scale simulation framework," *Journal of Parallel and Distributed Computing (in press)*, 2002.
- [13] "JavaSim," <http://javasim.cs.uiuc.edu>, 1999.
- [14] V. Jacobson, "Congestion avoidance and control," in *Proceedings of Conference on Applications, Technologies, Architectures, and Protocols for Computer Communications (SIGCOMM)*, 2001.
- [15] D. M. Chiu and R. Jain, "Analysis of the increase/decrease algorithms for congestion avoidance in computer networks," *Journal of Computer Networks and ISDN Systems*, vol. 17, no. 1, pp. 1–14, June 1989.
- [16] K. Fall and S. Floyd, "Simulation-based comparison of Tahoe, Reno, and Sack TCP," *Computer Communication Review*, vol. 26, pp. 5–21, 1996.
- [17] F. Gomes, "Optimizing incremental state-saving and restoration," Tech. Rep., Ph.D. thesis, Department of Computer Science, University of Calgary, 1996.
- [18] J. L. Lo, S. J. Eggers, J. S. Emer, H. M. Levy, R. L. Stamm, and D. M. Tullsen, "Converting thread-level parallelism to instruction parallelism via simultaneous multithreading," *Transactions on Computer Systems*, vol. 15, no. 3, pp. 322–354, 1997.
- [19] "Intel Pentium 4 and Xeon Processor Optimization Reference Manual," <http://developer.intel.com/design/pentium4/manuals/248966.htm>.
- [20] "Rocketfuel internet topology database," <http://www.cs.washington.edu/research/networking/rocketfuel>.
- [21] D. Nicol, "Scalability of network simulators revisited," in *Proceedings of Communication Networks and Distributed Systems Modeling and Simulation Conference (CNDS) part of Western Multi-Conference (WMC)*, 2003.
- [22] N. Spring, R. Mahajan, and D. Wetherall, "Measuring ISP topologies with Rocketfuel," in *Proceedings of Conference on Applications, Technologies, Architectures, and Protocols for Computer Communications (SIGCOMM)*, 2002.
- [23] D. Kotfila [kotfid@cs.rpi.edu](mailto:kotfid@cs.rpi.edu), "Personal communication," *Director, Cisco Academy, RPI*, 2002.
- [24] Z. Xiao, B. Unger, R. Simmonds, and J. Cleary, "Scheduling critical channels in conservative parallel discrete event simulation," in *Proceedings of the Workshop on Parallel and Distributed Simulation (PADS)*, 1999, pp. 20–28.
- [25] R. A. Meyer and R. L. Bagrodia, "Path lookahead: a data flow view of PDES models," in *Proceedings of the Workshop on Parallel and Distributed Simulation (PADS)*, 1999, pp. 12–19.
- [26] K. Perumalla, A. Ogielski, and R. Fujimoto, "Ted – a language for modeling telecommunication networks," in *Proceedings of ACM SIGMETRICS Performance Evaluation Review*, 1998, vol. 25.
- [27] B. J. Premore and D. M. Nicol, "Parallel simulation of TCP/IP using Ted," in *Proceedings of the Winter Simulation Conference (WSC)*, 1997, pp. 437–443.
- [28] B. Unger, Z. Xiao, J. Cleary, J.-J. Tsai, and C. Williamson, "Parallel shared-memory simulator performance for large ATM networks," *ACM Transactions on Modeling and Computer Simulation*, vol. 10, no. 4, pp. 358–391, 2000.
- [29] B. K. Szymanski, A. Saifee, A. Sastry, Y. Liu, and K. Madnani, "Genesis: A system for large-scale parallel network simulation," in *Proceedings of Workshop on Parallel and Distributed Simulation (PADS '02)*, 2002, pp. 89–96.